Communication

Organogel Formation by a Cholesterol-Stoppered Bistable [2]Rotaxane and Its Dumbbell Precursor

Yan-Li Zhao, Ivan Aprahamian, Ali Trabolsi, Natalia Erina, and J. Fraser Stoddart

J. Am. Chem. Soc., **2008**, 130 (20), 6348-6350 • DOI: 10.1021/ja800731k • Publication Date (Web): 30 April 2008

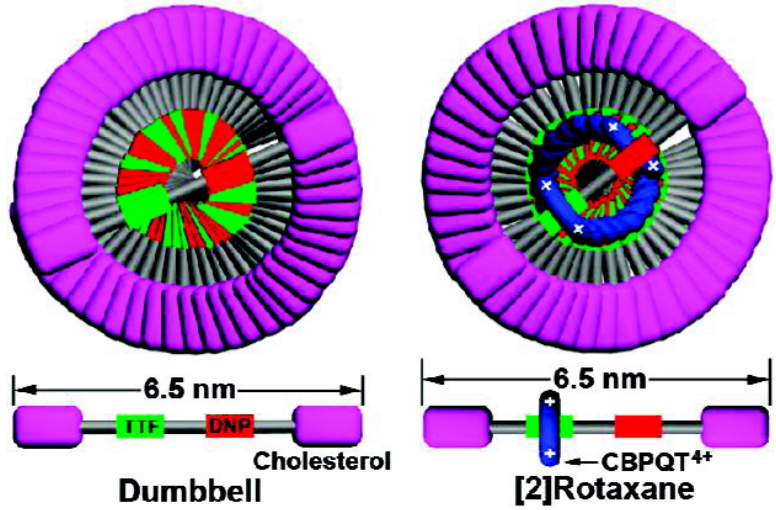

More About This Article

Additional resources and features associated with this article are available within the HTML version:

- Supporting Information
- Links to the 3 articles that cite this article, as of the time of this article download
- Access to high resolution figures
- Links to articles and content related to this article
- Copyright permission to reproduce figures and/or text from this article

View the Full Text HTML

J|A|C|S
COMMUNICATIONS

Published on Web 04/30/2008

Organogel Formation by a Cholesterol-Stoppered Bistable [2]Rotaxane and Its Dumbbell Precursor

Yan-Li Zhao,[†] Ivan Aprahamian,[†] Ali Trabolsi,[‡] Natalia Erina,[§] and J. Fraser Stoddart*,[‡]

Department of Chemistry and Biochemistry, University of California, Los Angeles, 405 Hilgard Avenue, Los Angeles, California 90095, Department of Chemistry, Northwestern University, 2145 Sheridan Road, Evanston, Illinois 60208, and Veeco Instruments, 112 Robin Hill Road, Santa Barbara, California 93117

Received January 29, 2008; E-mail: stoddart@northwestern.edu

Switchable rotaxanes[1,2] have attracted attention of late because of their ability to experience the relative movements of their ring and dumbbell components in response to external stimuli, such as pH or redox change and light. This mechanical property of these bistable molecules has been harnessed in a range of nanoelectromechanical devices, such as molecular muscle-activated cantilevers,[2c,3] macroscopic liquid transport,[4] molecular electronic devices,[5] and mesoporous silica-mounted nanovalves.[6] Recently, mechanically interlocked molecules have been found[7] to undergo self-organization, forming supramolecular aggregates of well-defined shapes and sizes. Bistable [2]rotaxanes with tetrathiafulvalene (TTF) and 1,5-dioxynaphthalene (DNP) recognition units situated in the rod portions of their dumbbell components and encircled by single cyclobis(paraquat-*p*-phenylene) ($CBPQT^{4+}$) rings have emerged[7] as one of the leading candidates for the formation of these supramolecular aggregates of well-defined sizes and shapes. In past situations, groups such as triisopropylsilane,[8] ferrocene,[9] and 3,5-diisopropylbenzene[10] and cores such as tetraarylmethane[1] and phloroglucinol[11] in hydrophobic and hydrophilic arrays have acted as stoppers in the TTF−DNP/$CBPQT^{4+}$-based rotaxanes and served different purposes. Herein, we describe the template-directed synthesis (Scheme 1), switching properties, gelation behavior, and self-organization of a cholesterol-stoppered bistable [2]rotaxane **1**·$4PF_6$ containing a $CBPQT^{4+}$ ring and TTF/DNP recognition units in its dumbbell component. It is well-known that cholesterol is a very efficient initiator of organogels[12] and liquid crystals.[13] We have introduced cholesterol as stoppers into **1**·$4PF_6$ in order to confer superstructural characteristics upon this bistable [2]rotaxane. We demonstrate that **1**·$4PF_6$ and precursor **2** both form organogels.

The dumbbell compound **2** was prepared (Scheme 1) in 68% yield by reaction of the diol **3**[1c] with cholesteryl chloroformate (**4**) and was then used to template the synthesis in 37% yield of **1**·$4PF_6$ with its $CBPQT^{4+}$ ring from its dicationic precursor[14] **5**·$2PF_6$ and 1,4-bis(bromomethyl)benzene (**6**). The bistable [2]rotaxane **1**·$4PF_6$ was isolated as an analytically pure green solid after SiO_2 column chromatography with a solution of NH_4PF_6 in Me_2CO as the eluent; it was characterized by NMR spectroscopy and electrospray ionization mass spectrometry.

The UV−vis spectrum (see Figure S5 in the Supporting Information [SI]) of **1**·$4PF_6$, recorded in CH_2Cl_2/MeOH (3:2), shows a broad transfer absorption band centered on 850 nm which is characteristic[1a] of the translational isomer in which the TTF unit is encircled by the $CBPQT^{4+}$ ring. No absorption band is observed in the 500−600 nm region for a charge transfer (CT) band which would result from the other translational isomer in which the DNP unit is encircled by the $CBPQT^{4+}$ ring, a fact which indicates that

Scheme 1. Template-Directed Synthesis of the Cholesterol-Stoppered Bistable [2]Rotaxane **1**·$4PF_6$

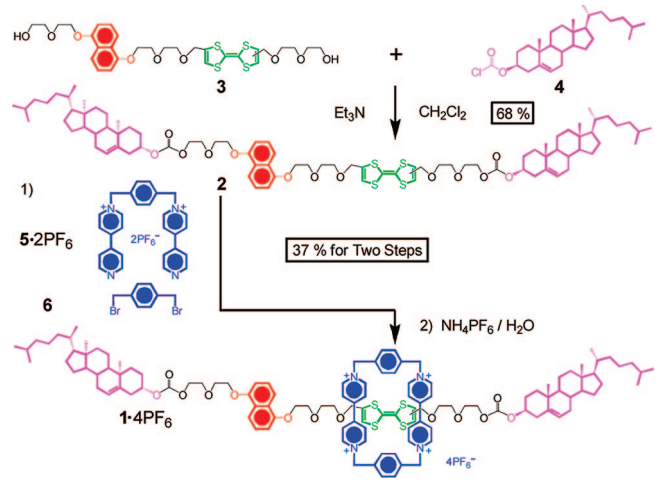

1·$4PF_6$ exists as predominantly a single translational isomer in solution—that is, one in which the $CBPQT^{4+}$ ring encircles the TTF unit. Thus, we can investigate the switching behavior of the $CBPQT^{4+}$ ring between the TTF and DNP units in **1**·$4PF_6$ by addressing the redox properties of the TTF unit. Switching was demonstrated using cyclic voltammetry (CV), differential pulse voltammetry (DPV), and UV−vis spectroelectrochemistry (SEC).

In the CV experiments (Figure 1), the dumbbell **2** exhibits two one-electron reversible oxidation processes at +0.36 and +0.80 V, characteristic[1c] of the first and second oxidation potentials of the TTF unit, respectively. DPV analysis revealed two oxidation peaks at +0.29 and +0.74 V. In the case of **1**·$4PF_6$, the first oxidation peak for the TTF unit which is discernible around +0.42 V for "free" TTF[1c,7] is hardly detectable at all in the anodic scan. DPV analysis shows (see Figure S6 in the SI) a small peak at +0.35 V. These results indicate that the existence of a whiff of "free" TTF is associated with a very small amount of the minor translational isomer present in **1**·$4PF_6$ at equilibrium. The first substantial TTF oxidation peak is shifted to higher potential and overlaps with the second oxidation peak at +0.76 V. In the DPV analysis, the first and second TTF oxidation peaks are found at +0.68 and +0.70 V, potentials which respectively correspond to the first oxidation of the TTF unit encircled by the $CBPQT^{4+}$ ring and the second oxidation of the TTF unit once the ring has migrated from the TTF to the DNP unit. In the cathodic scan carried out on **1**·$4PF_6$, two CV peaks, corresponding to the reduction of the oxidized $TTF^{\bullet+}$ radical cation and the TTF^{2+} dication, are respectively observed at +0.35 and +0.68 V, matching those of the dumbbell **2** at +0.29 and +0.72 V. This observation indicates that the $CBPQT^{4+}$ ring encircles the DNP unit, thus not affecting

[†] University of California, Los Angeles.
[‡] Northwestern University.
[§] Veeco Instruments.

10.1021/ja800731k CCC: $40.75

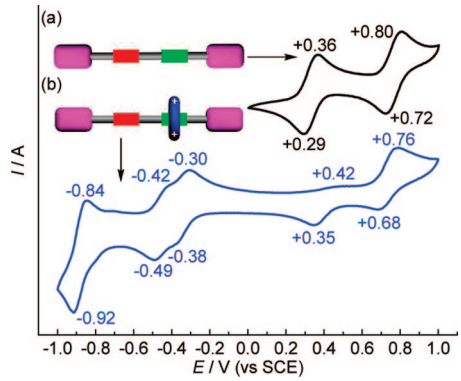

Figure 1. Cyclic voltammetry of (a) the dumbbell **2** (1.0 mM) and (b) the [2]rotaxane **1**·4PF$_6$ (1.0 mM) in 0.1 M TBA·PF$_6$ CH_2Cl_2/MeCN (1:1) solution at 25 °C with a scan rate of 200 mV s^{-1}.

the reduction potentials of the TTF^{2+} dication and the $TTF^{\bullet+}$ radical cation. In the reduction region of the CV of **1**·4PF$_6$, a typical splitting[1b,c,7,14] of the first two-electron reduction peak and no splitting of the second two-electron reduction peak of the $CBPQT^{4+}$ ring are observed. The splitting of the first reduction peak can be attributed to the electronic mixing from the CT interaction between the TTF unit and the $CBPQT^{4+}$ ring. The reductive portion of the DPV analysis reveals three peaks at −0.31, −0.41, and −0.84 V.

To shed further light on the mechanical movement of the $CBPQT^{4+}$ ring between the TTF and DNP unit, the switching in the bistable [2]rotaxane **1**·4PF$_6$ was investigated in solution by SEC (see Figure S8 in the SI). The ground state (E = 0 V) UV−vis spectrum of **1**·4PF$_6$ displays the characteristic CT band at 850 nm, corresponding to the CT interaction between the TTF unit and the $CBPQT^{4+}$ ring. The absorption spectrum starts to change on applying a potential of +0.40 V, and the ground state bands bleach and are replaced by bands in the visible region at 447 and 593 nm, associated with the absorption of the $TTF^{\bullet+}$ radical cation. These observations indicate that the $CBPQT^{4+}$ ring migrates away from the $TTF^{\bullet+}$ radical cation to the DNP unit during this process. When the applied potential is increased above +0.80 V, then the $TTF^{\bullet+}$ radical cation is oxidized to the TTF^{2+} dication. The absorption bands for the $TTF^{\bullet+}$ radical cation are bleached, and a small absorption peak at 520 nm, associated with the CT band between the DNP unit and the $CBPQT^{4+}$ ring, can be detected. The spectrum gradually changes back to its original form when the applied potential is switched off (E = 0 V) and the sample is left at rt for 24 h, indicating that all the electrochemical redox processes undergone by **1**·4PF$_6$ are fully reversible.

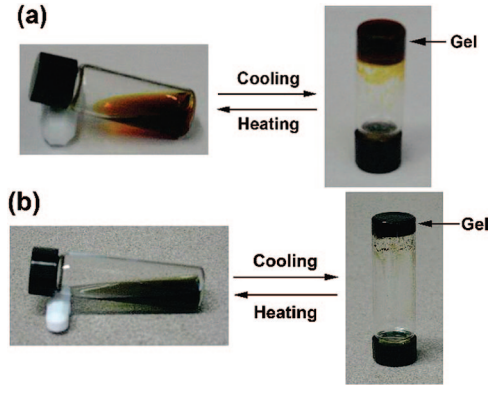

Figure 2. Sol−gel phase transition behavior of (a) the dumbbell **2** (0.5 M) and (b) the [2]rotaxane **1**·4PF$_6$ (0.8 M) in CH_2Cl_2/MeOH (3:2) solution when heating the temperature to 40 °C and cooling to 0 °C.

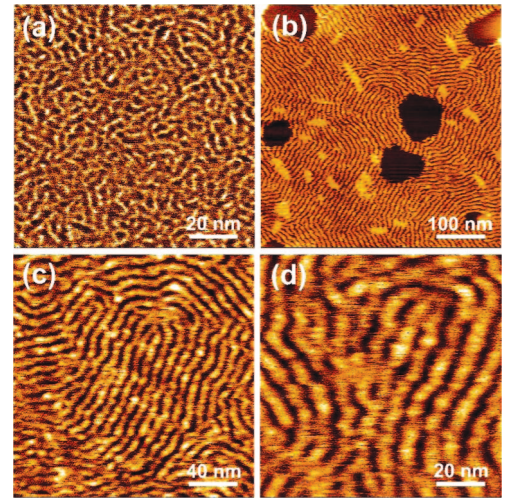

Figure 3. AFM images of the dumbbell **2** by (a) spin-casting CH_2Cl_2/MeOH (3:2) solution (5×10^{-5} M) and (b−d) nonsolvent deposition of the dumbbell **2** on HOPG substrates.

The gelation behavior of **1**·4PF$_6$ and **2** was investigated in a range of solvents. In most solvents, gels are not formed. We have found, however, that the CH_2Cl_2/MeOH (3:2) mixed solvent system sustains the gelation of both **1**·4PF$_6$ and **2**. Figure 2 illustrates the sol−gel phase transition that occurs when **1**·4PF$_6$ (0.8 M) and **2** (0.5 M) in CH_2Cl_2/MeOH (3:2) solution are heated to 40 °C and cooled to 0 °C. When $Fe(ClO_4)_3$ (>0.2 M, CH_2Cl_2/MeOH (3:2)) is brought into contact with the gels to oxidize the samples, the gels dissolve in the solution.

To obtain insight for the gelation behavior, the self-organization of **1**·4PF$_6$ and **2** was demonstrated by atomic force microscopy (AFM). On spin-casting a CH_2Cl_2 solution of **2** on an HOPG substrate, there is no evidence for self-organization (see Figure S9 in the SI). However, when spin-casting a CH_2Cl_2/MeOH (3:2) solution (5×10^{-5} M), or by nonsolvent deposition, of **2** on an HOPG substrate, linear superstructures can be seen to have formed (Figure 3) by AFM. The average width of the linear superstructures is 6.5 nm by section analysis. Similar observations have been made by AFM on **1**·4PF$_6$. Although no self-organization occurs on spin-casting a CH_2Cl_2 solution of **1**·4PF$_6$ on an HOPG substrate, linear superstructures are seen to have been formed (Figure 4) on spin-casting a CH_2Cl_2/MeOH (3:2) solution (5×10^{-5} M), or by nonsolvent deposition, of **1**·4PF$_6$ on HOPG substrates. The average width of the linear superstructures for **1**·4PF$_6$ is 6.0 nm. After $Fe(ClO_4)_3$ CH_2Cl_2/MeOH (3:2) solutions have been added to solutions of **1**·4PF$_6$ and **2** in the same solvent mixture, no self-organization was observed by AFM. We have also performed the AFM experiments by spin-casting highly concentrated solutions of **1**·4PF$_6$ (0.8 M) and **2** (0.5 M) on HOPG substrates. The concentrations we used in these experiments were close to the gelation conditions. Under these conditions, multiorganized rodlike or floccule aggregates can be observed (see Figures S11 and S14 in SI).

The circular dichroism (CD) spectra (see Figure S15 in the SI) of **1**·4PF$_6$ and **2**, recorded in CH_2Cl_2/MeOH (3:2) solutions, show negative (λ_{max} = 282 nm) and positive (λ_{max} = 295 nm) Cotton effects, respectively. These Cotton effects can be associated with the right and left-handed helical bias of the supramolecular self-organization chiralities[12i,15] generated by **1**·4PF$_6$ and **2**. The CD experiments provide important evidence for the supramolecular self-organization modes of **1**·4PF$_6$ and **2**, suggesting a helical molecular stacking in nature.

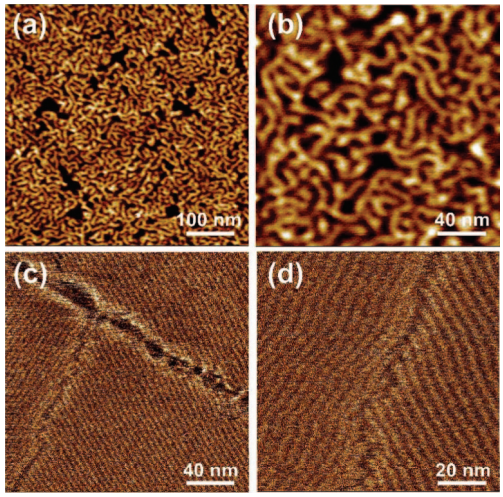

Figure 4. AFM images of the [2]rotaxane **1**·4PF_6 by (a and b) spin-casting CH_2Cl_2/MeOH (3:2) solution (5×10^{-5} M) and (c and d) nonsolvent deposition of the [2]rotaxane **1**·4PF_6 on HOPG substrates.

Molecular modeling of **1**·4PF_6 and **2** (using CERIUS2) shows that the molecular lengths of **1**·4PF_6 and **2** are both ~6.5 nm, in keeping with the experimental observations. According to the calculated and experimental results and the structural nature of **1**·4PF_6 and **2**, we propose the helical self-organization modes, shown respectively in panels a and b of Figure 5 for **1**·4PF_6 and **2** as follows: (1) random face-to-face stacking mode[12i,15,16] as a result of the packing of the cholesterol units and the $\pi-\pi$ interactions of the aromatic TTF and DNP units for **2**, and (2) alternate face-to-face stacking mode[12i,15,16] as a result of the packing of the cholesterol units and the $\pi-\pi$ interactions between the aromatic units in **1**·4PF_6 containing the charge-rich $CBPQT^{4+}$ ring. The proposed self-organization modes (Figure 5) explain the formation of linear superstructures of **1**·4PF_6 and **2**.

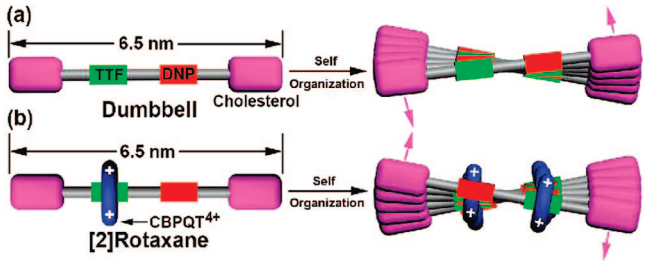

Figure 5. Possible self-organization modes of (a) the dumbbell **2** and (b) the [2]rotaxane **1**·4PF_6.

In summary, we have investigated the switching properties, gelation behavior, and self-organization of a cholesterol-stoppered bistable [2]rotaxane and compared it with its dumbbell precursor using spectroscopic, electrochemical, and microscopic methods. Organogels are formed by these two compounds in a CH_2Cl_2/MeOH (3:2) mixed-solvent system and liquified by adding an oxidizing agent. AFM shows that both compounds self-organize to form linear superstructures which we believe are helical in nature. The cholesterol stoppers are essential to this self-organization. This approach could be used as a general strategy for inducing self-organization by mechanically interlocked molecules.

Acknowledgment. We acknowledge support from the Microelectronics Advanced Research Corporation (MARCO) and its Focus Center Research Program (FCRP)—Center for Functional Engineered NanoArchitectonics (FENA), the Defense Advanced Research Projects Agency (DARPA), and the Center for Nanoscale Innovation for Defense (CNID).

Supporting Information Available: Experimental details and full list of authors for ref 14. This material is available free of charge via the Internet at http://pubs.acs.org.

References

(1) (a) Jeppesen, J. O.; Perkins, J.; Becher, J.; Stoddart, J. F. *Angew. Chem., Int. Ed.* **2001**, *40*, 1216. (b) Tseng, H.-R.; Vignon, S. A.; Stoddart, J. F. *Angew. Chem., Int. Ed.* **2003**, *42*, 1491. (c) Aprahamian, I.; Dichtel, W. R.; Ikeda, T.; Heath, J. R.; Stoddart, J. F. *Org. Lett.* **2007**, *9*, 1287.
(2) (a) Balzani, V.; Gómez-López, M.; Stoddart, J. F. *Acc. Chem. Res.* **1998**, *31*, 405. (b) Ballardini, R.; Balzani, V.; Credi, A.; Gandolfi, M. T.; Venturi, M. *Acc. Chem. Res.* **2001**, *34*, 445. (c) Collin, J.-P.; Dietrich-Buchecker, C.; Gaviña, P.; Jimenez-Molero, M. C.; Sauvage, J.-P. *Acc. Chem. Res.* **2001**, *34*, 477. (d) Kinbara, K.; Aida, T. *Chem. Rev.* **2005**, *105*, 1377. (e) Tian, H.; Wang, Q.-C. *Chem. Soc. Rev.* **2006**, *35*, 361. (f) Thomas, S. W., III; Joly, G. D.; Swager, T. M. *Chem. Rev.* **2007**, *107*, 1339. (g) Kay, E. R.; Leigh, D. A.; Zerbetto, F. *Angew. Chem., Int. Ed.* **2007**, *46*, 72.
(3) (a) Huang, T. J.; Brough, B.; Ho, C.-M.; Liu, Y.; Flood, A. H.; Bonvallet, P. A.; Tseng, H.-R.; Stoddart, J. F.; Baller, M.; Magonov, S. *Appl. Phys. Lett.* **2004**, *85*, 5391. (b) Liu, Y.; Flood, A. H.; Bonvallet, P. A.; Vignon, S. A.; Northrop, B. H.; Tseng, H.-R.; Jeppesen, J. O.; Huang, T. J.; Brough, B.; Baller, M.; Magonov, S.; Solares, S. D.; Goddard, W. A.; Ho, C.-M.; Stoddart, J. F. *J. Am. Chem. Soc.* **2005**, *127*, 9745.
(4) Berná, J.; Leigh, D. A.; Lubomska, M.; Mendoza, S. M.; Pérez, E. M.; Rudolf, P.; Teobaldi, G.; Zerbetto, F. *Nat. Mater.* **2005**, *4*, 704.
(5) Green, J. E.; Choi, J. W.; Boukai, A.; Bunimovich, Y.; Johnston-Halperin, E.; DeIonno, E.; Luo, Y.; Sheriff, B. A.; Xu, K.; Shin, Y. S.; Tseng, H.-R.; Stoddart, J. F.; Heath, J. R. *Nature* **2007**, *445*, 414.
(6) (a) Hernandez, R.; Tseng, H.-R.; Wong, J. W.; Stoddart, J. F.; Zink, J. I. *J. Am. Chem. Soc.* **2004**, *126*, 3370. (b) Nguyen, T. D.; Tseng, H.-R.; Celestre, P. C.; Flood, A. H.; Liu, Y.; Stoddart, J. F.; Zink, J. I. *Proc. Natl. Acad. Sci. U.S.A.* **2005**, *102*, 10029.
(7) Aprahamian, I.; Yasuda, T.; Ikeda, T.; Saha, S.; Dichtel, W. R.; Isoda, K.; Kato, T.; Stoddart, J. F. *Angew. Chem., Int. Ed.* **2007**, *46*, 4675.
(8) Bissell, R. A.; Córdova, E.; Kaifer, A. E.; Stoddart, J. F. *Nature* **1994**, *369*, 133.
(9) Benniston, A. C.; Harriman, A. *Angew. Chem., Int. Ed. Engl.* **1993**, *32*, 1459.
(10) Yu, H.; Beverly, K.; Stoddart, J. F.; Tseng, H.-R.; Heath, J. R. *Angew. Chem., Int. Ed.* **2003**, *42*, 5706.
(11) Jeppesen, J. O.; Perkins, J.; Becher, J.; Stoddart, J. F. *Org. Lett.* **2000**, *2*, 3547.
(12) (a) Murata, K.; Aoki, M.; Suzuki, T.; Harada, T.; Kawabata, H.; Komori, T.; Ohseto, F.; Ueda, K.; Shinkai, S. *J. Am. Chem. Soc.* **1994**, *116*, 6664. (b) Terech, P.; Weiss, R. G. *Chem. Rev.* **1997**, *97*, 3133. (c) Wang, R.; Geiger, C.; Chen, L.; Swanson, B.; Whitten, D. G. *J. Am. Chem. Soc.* **2000**, *122*, 2399. (d) Jung, J. H.; Ono, Y.; Shinkai, S. *Angew. Chem., Int. Ed.* **2000**, *39*, 1862. (e) van Esch, J. H.; Feringa, B. L. *Angew. Chem., Int. Ed.* **2000**, *39*, 2263. (f) Sugiyasu, K.; Fujita, N.; Shinkai, S. *Angew. Chem., Int. Ed.* **2004**, *43*, 1229. (g) Kawano, S.-i.; Fujita, N.; Shinkai, S. *J. Am. Chem. Soc.* **2004**, *126*, 8592. (h) Huang, X.; Terech, P.; Raghavan, S. R.; Weiss, R. G. *J. Am. Chem. Soc.* **2005**, *127*, 4336. (i) Ajayaghosh, A.; Vijayakumar, C.; Varghese, R.; George, S. J. *Angew. Chem., Int. Ed.* **2006**, *45*, 456. (j) Balaban, T. S.; Berova, N.; Drain, C. M.; Hauschild, R.; Huang, X.; Kalt, H.; Lebedkin, S.; Lehn, J.-M.; Nifaitis, F.; Pescitelli, G.; Prokhorenko, V. I.; Riedel, G.; Smeureanu, G.; Zeller, J. *Chem.—Eur. J.* **2007**, *13*, 8411. (k) Yagai, S.; Ishii, M.; Karatsu, T.; Kitamura, A. *Angew. Chem., Int. Ed.* **2007**, *46*, 8005. (l) Ajayaghosh, A.; Praveen, V. K. *Acc. Chem. Res.* **2007**, *40*, 644. (m) Tian, H.; Wang, S. *Chem. Commun.* **2007**, 781.
(13) (a) Hwang, J. J.; Iyer, S. N.; Li, L.-S.; Claussen, R.; Harrington, D. A.; Stupp, S. I. *Proc. Natl. Acad. Sci. U.S.A.* **2002**, *99*, 9662. (b) Mallia, V. A.; Tamaoki, N. *Chem. Soc. Rev.* **2004**, *33*, 76. (c) Abraham, S.; Mallia, V. A.; Ratheesh, K. V.; Tamaoki, N.; Das, S. *J. Am. Chem. Soc.* **2006**, *128*, 7692. (d) Mallia, V. A.; Vemula, P. K.; John, G.; Kumar, A.; Ajayan, P. M. *Angew. Chem., Int. Ed.* **2007**, *46*, 3269.
(14) Anelli, P.-L. et al. *J. Am. Chem. Soc.* **1992**, *114*, 193.
(15) (a) *Circular Dichroism: Principles and Applications*, 4th ed.; Berova, N., Nakanishi, K., Woody, R. W., Eds.; Wiley-VCH: Weinheim, Germany, 2000. (b) Cornelissen, J. J. L. M.; Fischer, M.; Sommerdijk, N. A. J. M.; Nolte, R. J. M. *Science* **1998**, *280*, 1427. (c) Engelkamp, H.; Middelbeek, S.; Nolte, R. J. M. *Science* **1999**, *284*, 785. (d) Hirschberg, J. H. K. K.; Brunsveld, L.; Ramzi, A.; Vekemans, J. A. J. M.; Sijbesma, R. P.; Meijer, E. M. *Nature* **2000**, *407*, 167. (e) Ma, X.; Wang, Q.; Qu, D.; Xu, Y.; Ji, F.; Tian, H. *Adv. Funct. Mater.* **2007**, *17*, 829. (f) Zhu, L.; Ma, X.; Ji, F.; Wang, Q.; Tian, H. *Chem.—Eur. J.* **2007**, *13*, 9216.
(16) Newkome, G. R.; Moorefield, C. N.; Baker, G. R.; Behera, R. K.; Escamillia, G. H.; Saunders, M. J. *Angew. Chem., Int. Ed. Engl.* **1992**, *31*, 917.

JA800731K